Proceedings of the 21st ICSMGE, Vienna, Austria, 14 – 19 June 2026. Pistrol, Adam & Schweiger (eds.)
Published by: ÖGG, Austrian Society for Geomechanics, Salzburg, Austria, ISBN 978-3-9503898-4-5
https://doi.org/10.53243/ICSMGE2026-1982

Effects Of Earthquake Motion Characteristics on Seismic Performance of Buried Pipes: An Experimental Study

Büşra Nur Kılınç
Sabanci Business School, Sabanci University, Istanbul, busra.kilinc@sabanciuniv.edu.tr

Ayşe Edinçliler
Kandilli Observatory and Earthquake Research Institute, Bogazici University, Istanbul

ABSTRACT: Buried pipelines are critical lifeline components whose seismic performance governs the reliability of water, gas, and sewerage networks. This study determines the response of buried High-Density Polyethylene (HDPE) pipes subjected to three earthquake motions with distinct peak accelerations and frequency characteristics through a series of 1-g shaking table tests conducted in a rigid-sided soil box. During the performing the experimental program, acceleration, lateral displacement, and surface settlement were measured to evaluate how input-motion features influence soil–pipe interaction. Test results showed that acceleration amplification ranged from 5–13% at pipe level and 14–20% near the surface, while pipe displacement exceeded table motion by 2–7%, depending on earthquake characteristics. Settlement varied between 0.35 and 0.43 cm, with the largest value produced by the El Centro earthquake acceleration record due to its broader frequency content. The results demonstrate that buried pipe response is governed by the combined effects of maximum acceleration and frequency characteristics, rather than peak acceleration alone. These findings provide experimentally validated insights for improving seismic design considerations for buried lifeline systems.

KEYWORDS: Buried pipes, HDPE pipes, shaking table, seismic response, soil–pipe interaction, earthquake motion characteristics

1 INTRODUCTION

Buried pipelines serve as the backbone of modern urban infrastructure, transporting water, sewage, gas, and other essential utilities. These critical lifeline systems are particularly vulnerable to seismic hazards, and their failure during earthquakes can result in catastrophic consequences including service disruptions, environmental contamination, and significant economic losses. Recent seismic events have demonstrated the vulnerability of buried pipeline systems, highlighting importance of comprehensive understanding of their seismic behavior.

The February 6, 2023, Kahramanmaras earthquakes with magnitudes of Mw= 7.7 and Mw =7.6 caused extensive damage to buried utilities across 13 provinces in Turkey, affecting over 14 million people (Toprak et al. 2024). Similar patterns of infrastructure damage have been observed in historical earthquakes including the 1999 Kocaeli earthquake, the 2011 Tohoku earthquake in Japan, and the 1994 Northridge earthquake in California. These events shows the critical importance of understanding how buried pipelines respond to different earthquake characteristics.

Compared to the traditional rigid pipes, high-density polyethylene (HDPE) pipes have gained widespread acceptance in modern infrastructure due to their superior properties including corrosion resistance, flexibility, lightweight nature, and cost efficiency. However, the seismic performance of HDPE pipes under various earthquake motions remains an active area of research requiring experimental validation.

Buried pipes are greatly affected by earthquakes and earthquake-induced phenomena including fault movement, landslides, ground deformation, and liquefaction. O'Rourke et al. (1999) described the deformations in pipes during earthquakes using two primary geotechnical mechanisms: temporary deformations due to the passage of seismic waves, and permanent deformations caused by fault ruptures, landslides, and liquefaction.

In linear pipes, deformations can be described as transverse and longitudinal. In longitudinal deformations, compression and tension are effective due to the propagation of seismic waves. The failure modes commonly observed in pipeline systems include joint failure, cracking, and buckling (Lanzano et al. 2013).

Buried pipelines are subjected to complex soil-structure interaction mechanisms during seismic events. The response of these systems depends on multiple factors including earthquake characteristics such as peak ground acceleration (PGA), frequency content, duration, and the dynamic properties of both the pipe and surrounding soil (O'Rourke & Liu, 1999; Lanzano et al. 2013). Understanding how different earthquake motion characteristics influence the seismic performance of buried pipes is essential for developing effective design guidelines and mitigation strategies.

Additional research has shown that the seismic response of buried pipelines varies substantially with soil type and soil–pipe interface behavior. Experimental and analytical studies indicate that clean sands and other cohesionless soils transmit seismic waves with limited damping, resulting in higher transient deformation demands on buried pipes (Alzabeebee 2019; Brachman et al. 2001). In contrast, cohesive soils may impose significant permanent ground movements during strong shaking, affecting the axial and bending response of pipelines as well as the performance of joints and connections (Bilgin & Stewart 2009). Classical interface studies such as Potyondy (1961) further demonstrate that soil–material friction plays a critical role in mobilizing resistance along the pipe surface, influencing both pullout and axial load transfer mechanisms. Numerical modeling efforts have also highlighted the importance of three-dimensional soil–pipe interaction under non-uniform seismic excitations (Sahoo et al. 2014). Broader evaluations of pipeline performance under seismic loading emphasize that soil type, burial conditions, and earthquake motion characteristics jointly govern the deformation mechanisms observed in buried lifeline systems (Toprak et al. 2007). Recent experimental and numerical studies have further expanded the understanding of ground failure mechanisms affecting buried pipelines. Large-scale model tests and coupled finite element and discrete element simulations showed that pipe bursts can trigger progressive seepage diffusion, erosion cavity formation, and eventual soil fluidization, leading to significant ground deformation and loss of support around the pipeline (Chao et al. 2025). Similarly, uplift and buoyancyrelated failures have been documented in saturated sands under liquefaction, where buried pipes experience upward displacement due to excess pore pressure generation and reduced effective stress (Pal et al. 2011). In addition to vertical instability mechanisms, longitudinal non-uniform excitations can induce substantial axial strain accumulation along continuous pipelines, especially when spatial variability in input motion amplifies bending and tension demands (Zhang et al. 2024). Together, these studies highlight that buried pipeline performance is strongly influenced not only by seismic wave characteristics but also by complex soil deformation modes such as erosion, buoyancy-driven uplift, and spatially varying dynamic loads.

This study aims to investigate the seismic behavior of buried HDPE pipes through a comprehensive experimental program using shaking table tests. The research focuses specifically on understanding how earthquake motion characteristics affect the acceleration, displacement, and settlement responses of buried pipeline systems. In particular, the study evaluates how differences in earthquake characteristics (acceleration, frequency content and time) of the selected earthquake records influence acceleration and displacement responses, thereby clarifying the relationship between input motion characteristics and the seismic deformation response of buried pipelines.

2 EXPERIMENTAL PROGRAM

2.1 *Test facility and setup*

The experimental program was conducted at the shaking table system consists of a 3m × 3m platform capable of generating horizontal vibrations with a maximum force of 2g and total lateral displacement of 24 cm (±12 cm).

A specially designed rigid steel soil box with inner dimensions of 90 cm (width) × 120 cm (length) × 90 cm (height) was used for the experiments. Soil box front view and side view are given in Figure 1. The soil box was specifically manufactured for seismic performance tests of buried pipes. Before starting to sample preparation in the plexiglass rigid box, the inner surfaces are coated with grease oil to better simulate field conditions, reduce wave reflections, and minimize boundary effects.

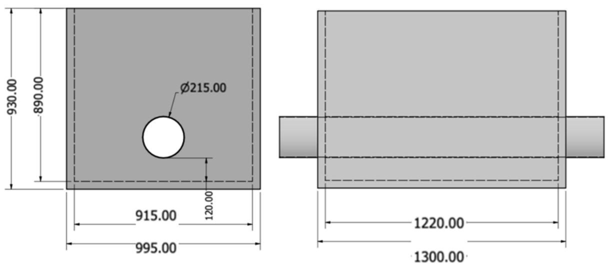

Figure 1 Soil box front view and side view with dimensions (mm).

2.2 *Soil properties and pipe specifications*

"Silivri Sand" which refers to the natural sand material collected from the Silivri district of Istanbul, was used as the soil medium throughout the experimental program. The grain size distribution of sand, determined according to ASTM Standards D422 and D6913, is shown in Figure 1. The uniformity coefficient (C_u) is 2.68, the curvature coefficient (C_c) is 1.06, and the D_{50} value is 0.3. According to the United Soil Classification System (USCS), Silivri sand is classified as poorly graded sand (SP), with a bulk unit weight of 16.5 kN/m³, and internal friction angle of 24° as shown in Table 1. The sand was placed and compacted within the soil box to achieve a relative density of about 60% for all tests. To promote uniform packing, each layer was compacted following a controlled procedure, including the application of a 9 Hz vibration, in accordance with Bathurst et al. (2007). Before each shaking table test, the soil box was completely emptied and refilled, and the same placement and compaction procedure was strictly repeated to ensure consistent initial density conditions. In other words, a new experimental setup was prepared for each test model and sample preparation was repeated for each model (Kılınç, 2024).

Table 1. Soil properties.

Parameter	Symbol	Value	Unit
Unit weight	γ	16.5	kN/m^3
Specific gravity	*Gs*	2.7	-

The tests employed a high-density polyethylene (HDPE) pipe with an internal diameter of 200 mm, an outer diameter of 215 mm, and a wall thickness of 7.5 mm, corresponding to an elastic modulus of 1000 MPa. The pipe was placed 120 mm above the base of the soil box, consistent with typical burial depths for small-diameter utility pipes.

2.3 *Instrumentation and earthquake motions*

The experimental setup included comprehensive instrumentation to capture the dynamic response of the soil-pipe system. A total of 16 accelerometers were strategically placed throughout the test setup, including locations on the shaking table (A1), on the pipe at various locations (A5, A7, A8, A9), and embedded in soil at different depths (A6, A10-A16) as shown in Figure 2. Five Linear Variable Differential Transformers (LVDTs) and one potentiometer were used to measure displacements at critical locations. D17 (potentiometer) was mounted on the shaking table to measure input displacement. D20 and D21 (LVDTs) were positioned at the two pipe outlets to measure lateral pipe displacement. D19 (LVDT) was placed on the soil surface directly above the pipe centerline to continuously measure vertical surface settlement during shaking, with post-test verification using a precision ruler at multiple surface points. D18 and D22 (LVDTs) were positioned on the soil box wall and inside the pipe, respectively, for supplementary measurements. All instruments were calibrated prior to testing, and data were recorded at a sampling rate of 200 Hz.

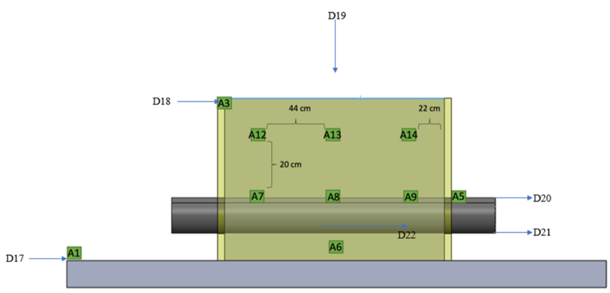

Figure 2. Instrumentation Plan for Shaking Table Models.

For the experimental program, three earthquake records with different characteristics were selected to evaluate the influence of earthquake motion parameters on buried pipe response (Table 2). These earthquake records were selected to provide a range of peak ground accelerations and frequency characteristics, enabling assessment of how different earthquake parameters influence buried pipe response. The

1999 Kocaeli earthquake acceleration record represents low-intensity, low-frequency excitation; The 1940 El Centro earthquake acceleration record represents moderate-intensity, intermediate-frequency content; and the 1995 Kobe earthquake acceleration record represents high-intensity, high-frequency excitation with broad spectral characteristics. The raw input motions corresponding to the stations listed in Table 2 are shown in Figures 3–5 through their acceleration–time histories and Fourier amplitude spectra.

Table 2. Earthquake motions

Earthquake name	Station	PGA (g)	Frequency (Hz)	Magnitude (Mw)	Rjb (km)	Vs30 (m/s)
Kocaeli – İznik (1999)	Iznik	0.15	0.66	7.5	15	690
El-centro (1940)	Imperial Valley	0.3	1.2	6.9	16.9	230
Kobe (1995)	KJMA	0.82	1.48	6.9	1	312

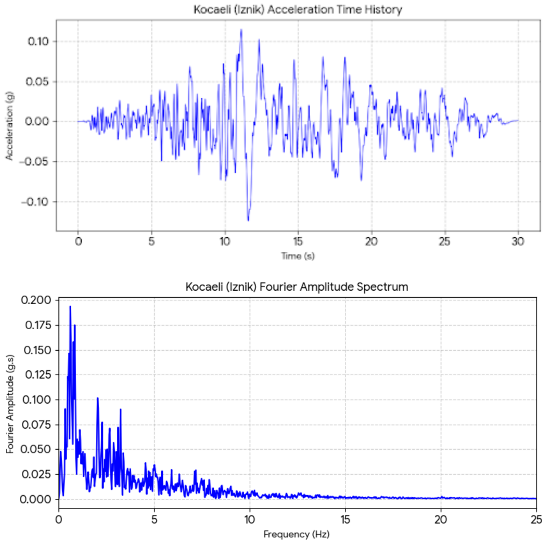

Figure 3. Kocaeli Earthquake İznik Station Acceleration Record

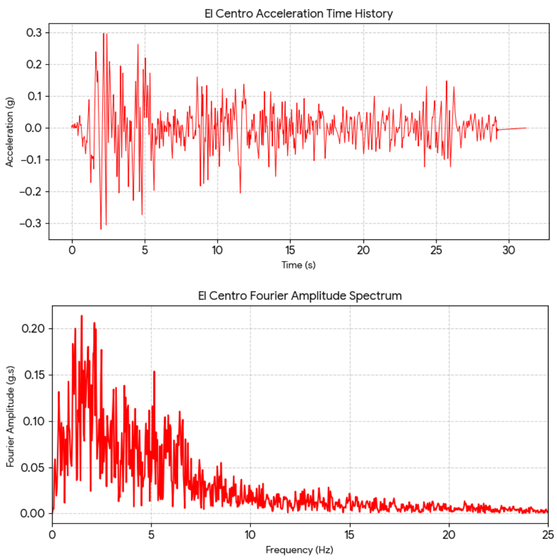

Figure 4. El-Centro Earthquake Imperial Valley Station Acceleration Record.

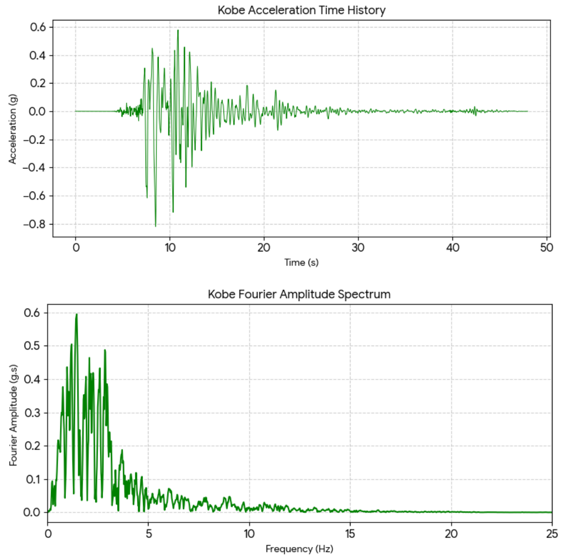

Figure 5. Kobe Earthquake KJMA Station Acceleration Record.

EXPERIMENTAL RESULTS

2.4 *Acceleration response*

The acceleration responses recorded during the experiments reveal significant insights into how earthquake characteristics influence the seismic behavior of buried pipe systems. Figures 6, 7, and 8 present the acceleration time-history responses measured at important locations: shaking table (A1), pipe level (A7), and near-surface (A14) for all three earthquake motions.

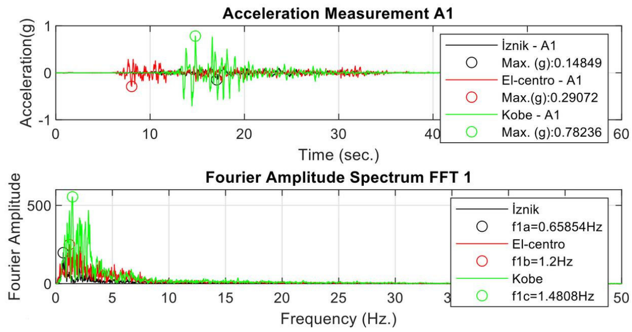

Figure 6. Time-history and fourier amplitude spectrum graphs for A1.

Under the Kocaeli earthquake motion (PGA = 0.15g), the maximum acceleration recorded at the shaking table (A1) was 0.149g. The pipe-level accelerometer (A7) recorded a maximum acceleration of 0.156g, representing a 5% amplification compared to the input motion. The near-surface accelerometer (A14) showed more significant amplification, reaching 0.169g, which represents a 14% increase over the input motion.

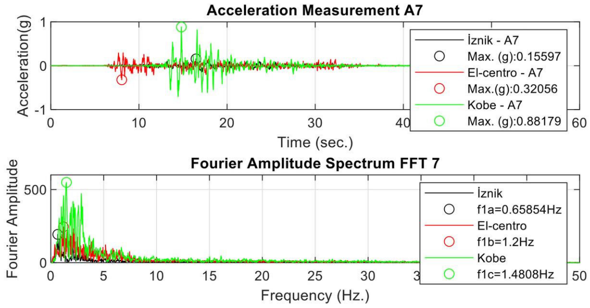

Figure 7. Time-history and fourier amplitude spectrum graphs for A7.

The moderate amplification observed during the Kocaeli earthquake (5% at pipe level, 14% at surface) indicates that low-intensity seismic motions are transmitted through the soil medium with depth-dependent amplification patterns. The greater amplification near the surface suggests that shallow soil layers contribute to motion amplification effects.

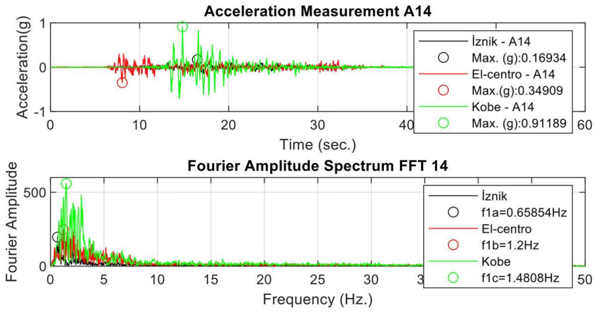

Figure 8. Time-history and fourier amplitude spectrum graphs for A14.

The El-Centro earthquake motion (PGA = 0.30g) produced more pronounced acceleration responses throughout the system. The input motion with a maximum acceleration of 0.291g was amplified to 0.321g at the pipe level (A7), representing a 10% increase. The surface-level accelerometer (A14) recorded as 0.349g, showing a 20% amplification.

The high-intensity Kobe earthquake motion (PGA = 0.82g) exhibited the largest absolute acceleration values but moderate relative amplification. The input motion of 0.782g was amplified to 0.882g at the pipe level (13% increase) and 0.912g near the surface (17% increase). Despite the large peak accelerations, the resulting surface amplification (17%) was smaller than that produced by the El-Centro input motion (20%).

2.5 *Displacement and settlement analysis*

2.5.1 *Lateral displacement patterns*

The lateral displacement measurements provide insights into the relative motion between the soil, pipe, and shaking table during seismic excitation. The El Centro earthquake motion produced the largest pipe displacement of 9.83 cm, followed by the Kobe earthquake motion with 9.25 cm, and the Kocaeli earthquake motion with 7.66 cm as shown in Figure 9. The displacement values show a general trend of increasing with peak ground acceleration. However, the Kobe motion (PGA = 0.82g, displacement = 9.25 cm) produced slightly lower displacement than the El Centro motion (PGA = 0.30g, displacement = 9.83 cm).

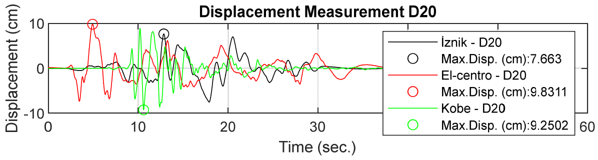

Figure 9. The displacement measurements of D20.

The shaking table displacement measurements (D17) are presented in Figure 10, showing maximum displacement of 9.52 cm under the El-Centro earthquake motion. Comparative analysis of pipe and shaking table displacements reveals important soil-pipe interaction characteristics. Under the El-Centro earthquake motion, the pipe displacement (9.83 cm) exceeded the shaking table displacement (9.52 cm) by 3% as shown in Figure 10. Similarly, the Kobe earthquake motion resulted in a 7% increase in pipe displacement relative to the input motion, while the Kocaeli earthquake motion showed a 2% increase.

These findings indicate that the buried pipe system experiences displacement amplification during seismic excitation, with the value of amplification varying based on earthquake characteristics. The higher amplification observed under the Kobe earthquake motion suggests that frequency content and acceleration characteristics influence the dynamic coupling between the pipe and surrounding soil.

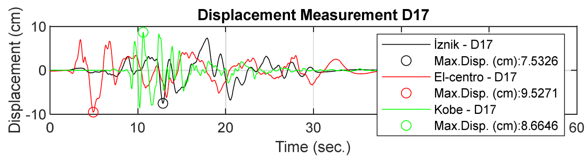

Figure 10. The displacement measurements of D17.

2.5.2 *Settlement of the soil surface*

Vertical dislapcements of te soil surface provides an indication of soil densification during seismic loading. Settlement was measured using the LVDT (D19) shown in Figure 2, positioned above the soil surface to capture vertical displacement during shaking. The largest settlement occurred under the El Centro earthquake motion, measuring 0.43 cm. The Kobe earthquake motion produced settlement of 0.37 cm, while the Kocaeli earthquake motion resulted in minimal settlement of 0.35 cm as shown in Figure 11. The settlement patterns exhibit correlation with both intensity and spectral characteristics of the input motions. Although the El Centro earthquake motion had only a moderate PGA (0.30g), it generated the largest settlement because its wider frequency content caused greater soil densification during shaking.

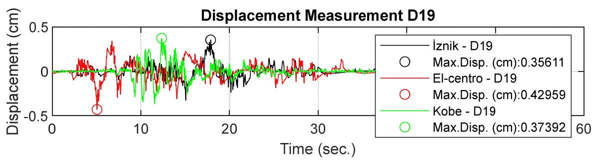

Figure 11. The vertical displacement measurements of D19.

2.6 *Frequency response analysis*

The Fourier amplitude spectra clearly show the frequency content unique to each earthquake motion, as presented in Figures 3–5. The Kocaeli earthquake motion exhibits dominant frequencies in the range of 1-3 Hz, while the El Centro earthquake motion shows broader frequency content with significant energy between 0.5-5 Hz. The Kobe earthquake motion demonstrates the most distributed frequency content with energy spread across a wider frequency range, showing multiple peaks and broader spectral characteristics compared to the other earthquake motions.

The Fourier amplitude spectra reveal the frequency characteristics of the soil-pipe system response. In Figures 6-8, the dominant frequencies remain consistent across all measurement locations (A1, A7, and A14): 0.66 Hz for Kocaeli, 1.2 Hz for El Centro, and 1.48 Hz for Kobe earthquakes. This consistency indicates that the dominant frequency of the input motion is transmitted through the soil-pipe system without significant alteration.

3 DISCUSSION

The experimental results are interpreted herein with respect to the primary earthquake motion characteristics as peak ground acceleration and frequency content on experimental system response.

3.1 *Effect of peak ground acceleration*

The experimental results demonstrate that peak ground acceleration significantly influences the absolute magnitude of acceleration and displacement responses in buried pipe systems. However, the relationship between PGA and response amplification is not linear. The amplification factors observed range from 5-14% for pipe-level accelerations and 14-20% for surface-level accelerations.

The moderate-intensity El Centro earthquake motion (PGA = 0.30g) produced the highest relative amplification (20% at surface), while the high-intensity Kobe earthquake motion (PGA = 0.82g) showed more moderate amplification (17% at surface). This suggests that soil behavior and soil-pipe interaction effects may be influenced by nonlinear mechanisms at higher acceleration levels.

3.2 *Frequency content effects*

Th frequency-domain analysis shows that the dominant frequency components of the input motions are consistently transmitted through the soil profile. The spectral shapes remain largely unchanged with depth, indicating that the soil layer does not significantly filter or distort the fundamental frequency content of the applied excitations. Accordingly, each input motion retains its characteristic dominant frequency throughout the system. This spectral consistency reflects effective dynamic coupling between the shaking table, the soil deposit, and the buried pipe. The results further demonstrate that the dominant frequency content is governed by the characteristics of the input motion and remains independent of the PGA level (0.15 g, 0.30 g, and 0.82 g for Kocaeli, El Centro, and Kobe earthquake motions, respectively). Overall, the experimental setup successfully preserves the primary frequency characteristics of each earthquake motion across the model depth.

4 CONCLUSIONS

This study experimentally assessed the seismic response of buried HDPE pipes subjected to three earthquake motions with varying peak accelerations and frequency characteristics. The main findings are as follows:

Acceleration amplification increased with depth toward the ground surface, ranging from 5–13% at pipe level and 14–20% near the soil surface, reflecting depth-dependent wave propagation effects in the soil.

The response was nonlinear: although Kobe earthquake motion had the largest PGA, the El Centro earthquake motion produced the highest amplification. This shows that amplification is not governed by PGA alone, but also by frequency.

Lateral displacement measurements showed that the buried pipe experienced 2–7% displacement amplification relative to the input motion. Pipe displacement was influenced by both peak acceleration and frequency content, with the largest displacement recorded under the El Centro earthquake motion.

The dominant frequencies of the input motions were consistently transmitted through the soil-pipe system. The spectral response remained stable across the depths, suggesting effective dynamic coupling without significant filtering within the tested frequency range.

Vertical displacements ranged from 0.35 cm to 0.43 cm were affected by duration of shaking. The El Centro earthquake motion produced the greatest settlement due to its wider frequency content.

Overall, the results demonstrate that the seismic performance of the buried HDPE pipes is governed by the frequency content, rather than maximum acceleration alone. These findings provide useful reference data for validating numerical soil–pipe interaction models and support the development of improved seismic design considerations for buried lifeline systems.

Further work should investigate how variations in burial depth, pipe diameter, and soil type modify the seismic response observed in this study. Expanding the test program to include earthquake records with broader frequency content and longer durations would allow more comprehensive evaluation of input-motion effects. In parallel, numerical models calibrated against the present experimental data can be used to examine soil–pipe interaction under a wider range of seismic loading scenarios.

5 ACKNOWLEDGEMENTS

The authors acknowledge the support provided by Boğaziçi University Research Fund Grant Number BAP14020. The authors also thank Superlit Company for providing the HDPE pipes used in the experiments.

6 REFERENCES

Alzabeebee, S. 2019. Seismic response and design of buried concrete pipes subjected to soil loads. *Tunnelling and Underground Space Technology* 93, 103084.

Anderson, C., Wijewickreme, D., Ventura, C., and Mitchell, A. 2005. Full-scale laboratory testing of soil-pipe interaction in branched polyethylene pipelines. *Experimental Techniques* 29(2), 33-37.

Bilgin, Ö., and Stewart, H. E. 2009. Pullout resistance characteristics of cast iron pipe. *Journal of Transportation Engineering* 135, 730-735.

Brachman, R. W., Moore, I. D., and Rowe, R. K. 2001. The performance of a laboratory facility for evaluating the structural response of small-diameter buried pipes. *Canadian Geotechnical Journal* 38(2), 260-275.

Chao, H., Tan, Y., & Su, Z.-K. (2025). *Ground failure and soil erosion caused by bursting of buried water pipeline: Experimental and numerical investigations.* Engineering Failure Analysis, 167, 108965.

Chian, S. C., Tokimatsu, K., and Madabhushi, G. 2014. *Soil liquefaction-induced uplift of underground structures: physical and numerical modeling.* Cambridge University Press.

Eid, H. T., Al-Nohmi, N. M., Wijewickreme, D., and Amarasinghe, R. S. 2019. Drained peak and residual interface shear strengths of fine-grained soils for pipeline geotechnics. *Journal of Geotechnical and Geoenvironmental Engineering* 145(6), 04019026.

Kılınç, B.N., 2024. Effects of geosynthetic reinforcement on the seismic performance of buried pipes. Master's thesis. Bogazici University.

Lanzano, G., Salzano, E., Santucci de Magistris, F., and Fabbrocino, G. 2013. Seismic vulnerability of gas and liquid buried pipelines. *Journal of Loss Prevention in the Process Industries* 26, 72-78.

O'Rourke, M. J., and Liu, X. 1999. *Response of buried pipelines subject to earthquake effects.* MCEER, Buffalo, NY.

O'Rourke, M. J., Jeon, S. S., Toprak, S., Cubrinovski, M., Hughes, M., van Ballegooy, S., and Bouziou, D. 1999. Earthquake response of underground pipeline networks in Christchurch, NZ. *Earthquake Spectra* 30(1), 183-204.

Pal, S. K., Dasgupta, S., & Sengupta, A. (2011). *Uplift behaviour of buried pipeline in liquefied soil: Experimental and theoretical studies.* Tunnelling and Underground Space Technology, 26(3), 460–467.

Potyondy, J. G. 1961. Skin friction between various soils and construction materials. *Géotechnique* 11(4), 339-353.

Sahoo, S., Manna, B., and Sharma, K. G. 2014. Seismic behaviour of buried pipelines: 3D finite element approach. *Journal of Earthquakes* 2014, 818923.

Sarvanis, G. C., Karamanos, S. A., Vazouras, P., Mecozzi, E., Lucci, A., and Dakoulas, P. 2018. Permanent earthquake-induced actions in buried pipelines: numerical modeling and experimental verification. *Earthquake Engineering & Structural Dynamics* 47(4), 966-987.

Toprak, S., Kosar, K., Nacaroglu, E., and O'Rourke, M. J. 2007. Seismic response of buried pipelines. *Geotechnical Earthquake Engineering and Soil Dynamics IV* 1-10.

Toprak, S., Wham, B., Nacaroglu, E., Ceylan, M., Dal, O., and Senturk, A. E. 2024. The effects of February 6, 2023 Kahramanmaras earthquakes on pipelines. *18th World Conference on Earthquake Engineering*, Milan, Italy.

Wang, L. R. L., and Zhang, H. 1992. Buried pipeline system in a liquefaction environment. *Proc. 10th World Conference on Earthquake Engineering*, Madrid, Spain.

Yan, K., Zhang, J., Wang, Z., Liao, W., and Wu, Z. 2018. Seismic responses of deep buried pipeline under non-uniform excitations from large scale shaking table test. *Soil Dynamics and Earthquake Engineering* 109, 180-192.

Zhang, Z., Zhang, X., & Zhang, J. (2024). *Seismic response of buried pipelines under longitudinal non-uniform ground motions: Shaking table study and numerical modeling.* Soil Dynamics and Earthquake Engineering, 183, 107874.